arXiv:1412.2025v2 [astro-ph.CO] 9 Jan 2015

KINEMATIC EFFECTS OF THE VELOCITY FLUCTUATIONS FOR DARK HALOS POPULATION IN ΛCDM MODEL

E. P. Kurbatov

Institute of astronomy, Russian Academy of Sciences

48 Pyatnitskaya st., Moscow, Russian Federation, 119017

kurbatov@inasan.ru

Abstract

ΛCDM-model predicts an excess of dark halos compared to the observations. The excess is seen from the estimates of the virialized mass inside the Local Supercluster and its surroundings. It is shown that account for cosmological velocity fluctuations in the process of formation of the population of dark halos it is possible to eliminate this contradiction remaining within the framework of the ΛCDM cosmology. Based on the formalism of Press and Schechter, we suggest a model of formation of dark halo population which takes into account the kinematic effects in the dark matter. The model allows a quantitative explanation for the observable deficit of the virialized mass in the local Universe.

1. Introduction

The inconsistencies between the predictions of the ΛCDM cosmological model and the observations concern the distribution of the matter on the scales smaller than the scale of homogeneity of the Universe. In particular, note the deficit of virialized matter in the local Universe (Makarov and Karachentsev 2011). Counts of the mass of the galaxies, virialized groups, and clusters of galaxies in the Local Supercluster and its environs performed by many authors revealed the lack of mass inside the virialized objects, amounting to a half of an order of magnitude (see the references in Makarov and Karachentsev (2011)). According to the Makarov and Karachentsev (2011) catalog the estimate of the local density parameter inside a sphere of the radius 48 Mpc is about 0.08 ± 0.02. As a possible explanation of this deficit Makarov and Karachentsev (2011) suggested that about 2/3 of the matter is located outside the virialized areas. Instead, this dark matter is either concentrated in dark clumps, outside the virial regions, or distributed diffusively. In the favor of the idea of the dark clumps tell observational data on weak lensing (Jee et al. 2005) and on disturbed galaxies (Karachentsev et al. 2006).

One of the generally accepted ideas on the Large-Scale Structure formation in the Universe is the hierarchical model. Formation of the virialized halos population in the ΛCDM model is represented

as a continuous process of condensing and clustering of the structures which develop from the density perturbations. Stochastic nature of this process is determined by the properties of the initial cosmological fluctuations. As a result, a hierarchical halos structure forms, which consists of galactic clusters, virialized groups, field galaxies and low-mass satellite galaxies. Press and Schechter (1974) suggested a simple model for evolution of the dark halos mass function. Development of this model in later studies helped to solve the problem to a good approximation. The extension of the PS model known as the Excursion-Set or the Extended PS (EPS) formalism (Bond et al. 1991; Lacey and Cole 1993) is based on two assumptions: (i) the requirement for the perturbation to be virialized at a given time which can be formulated in the terms of the density perturbation field at the linear stage of its evolution; (ii) the mass function of halos is formulated for those objects which are at the top of the hierarchical structure, i.e. they do not belong to other halos. In this formulation, the problem can be solved using the linear perturbation theory only.

In the formation process of the dark halos population the environment effects, which can lead to the loss of the halo mass or to the ejection of the sub-halos from the parent clusters, have an essential importance. In the numerical model of Diemand et al. (2007) was shown that the most intensive loss of sub-halo happens before virialization of the parental halo. An already formed halo can accumulate up to 20% of its mass by the accretion of surrounding dark matter.

Despite of the quite obvious role of the environment effects, they are not the only ones which are able to influence the halo population. For instance, Valageas (2012) have shown that the velocity fluctuations in the dark matter (the author considered the Warm Dark Matter model, WDM) can affect the density fluctuations statistics on scales $\lesssim 0.1h^{-1}$ Mpc. Valageas (2012) did not find any considerable effect of the velocity fluctuations for the dark halos population. It should be emphasized however that the calculations were constrained to corrections to the power spectrum only. More, approach used in the latter study required modification of the ΛCDM-model.

An interesting problem is the possibility of direct kinematic effect of the velocity fluctuations on the process of the formation of the individual halos as well as their population. It is well known that the velocity fluctuations grow along to the density fluctuations (Crocce and Scoccimarro 2006). Due to the moment conservation, the halo during formation process inherits velocity of the dark matter averaged over its scale. When this halo becomes involved in the formation process of the larger scale gravitational condensation, its velocity may be large enough to leave the parental structure. This effect may change the history of evolution of dark halos, the dark halos population itself, as well as the history of the chemical evolution of the galaxies.

In this paper, a method for accounting for the kinematic effects in the dark halos population process is suggested. The evolutionary model of the population is formulated on the base of the Excursion-Set theory (Bond et al. 1991; Lacey and Cole 1993) in terms of kinetic equation. Also, the problems of the choice of the initial conditions and of the influence of the background structure are considered.

In § 2 the EPS model is briefly examined. In § 3 formation model for individual halo with

kinematic effects is suggested and the kinetic equation for the mass function is obtained. In § 4 the model is applied to the problem of the virialized mass deficit in the local Universe. Conclusions are presented in § 5.

2. Formation of the halo population in the EPS model

2.1. Growth of the cosmological perturbations

In the ΛCDM model the Large-Scale Structure of the Universe is formed from the growing fluctuations of density and velocity in the cold dark matter. Evolution law of the structures with characteristic mass m can be linked to the properties of the overdensity field $\delta \equiv (\rho - \rho_{\rm cr,0})/\rho_{\rm cr,0}$ averaged over the volume containing mass m. The averaging is defined as a convolution of the field with a filter W:

$$\delta(a, \mathbf{x}, m) = \int d^3x'\, W(\mathbf{x}' - \mathbf{x}, m)\, \delta(a, \mathbf{x}') \;, \tag{1}$$

where a is the scale factor, which is related to the redshift z as $a = 1/(z+1)$; m is the halo mass. The same in the terms of the Fourier transform is[1]:

$$\tilde{\delta}(a, \mathbf{k}, m) = (2\pi)^{3/2}\, \tilde{W}(\mathbf{k}, m)\, \tilde{\delta}(a, \mathbf{k}) \;. \tag{2}$$

The „top-hat“ filter will be adopted hereinafter:

$$W(\mathbf{x}, m) = \frac{3}{4\pi X^3}\, \theta(X - x) \;, \tag{3}$$

$$(2\pi)^{3/2}\, \tilde{W}(\mathbf{k}, m) = 3\, \frac{\sin kX - kX \cos kX}{k^3 X^3} \;, \tag{4}$$

where $X = [3m/(4\pi\Omega_{\rm m,0}\rho_{\rm cr,0})]^{1/3}$.

The random fluctuations field is assumed to be Gaussian with zero mean and delta-correlated over Fourier modes,

$$\langle \tilde{\delta}(a, \mathbf{k})\, \tilde{\delta}^*(a, \mathbf{k}') \rangle = \delta_{\rm D}(\mathbf{k} - \mathbf{k}')\, P(a, k) \;, \tag{5}$$

where $\delta_{\rm D}$ is the Dirac's delta-function, $P(a, k)$ is the overdensity power spectrum at the moment corresponding to the scale factor a. Thereby, over spatial scale associated with the given mass m the overdensity field can be characterized by only the variance value, which is independent of spatial position:

$$S(a, m) \equiv \langle \delta^2(a, \mathbf{x}, m) \rangle = \int d^3k\, |\tilde{W}(\mathbf{k}, m)|^2\, P(a, k) \;. \tag{6}$$

Velocity divergence fluctuations field $\theta \equiv \nabla_{\mathbf{x}}(a\dot{\mathbf{x}})$ has the same properties:

$$\langle \tilde{\theta}(a, \mathbf{k})\, \tilde{\theta}^*(a, \mathbf{k}') \rangle = \delta_{\rm D}(\mathbf{k} - \mathbf{k}')\, P_\theta(a, k) \;, \tag{7}$$

[1]The Fourier transform is defined as $\tilde{f}(\mathbf{k}) = (2\pi)^{-3/2} \int d^3x\, e^{i\mathbf{kx}} f(\mathbf{x})$.

where $P_\theta(a,k)$ is the power spectrum of the field $\theta(a,\mathbf{x})$. Let denote as $\mathbf{v} \equiv a\dot{\mathbf{x}}$ the field of the physical velocity determined relatively to the expanding Universe. We neglect the vortical part of the velocity fluctuations. In this case, the velocity field is determined by the divergence field only:

$$\langle\tilde{\theta}(a,\mathbf{k})\,\tilde{\theta}^*(a,\mathbf{k}')\rangle = \sum_{j,j'} k_j k'_{j'}\,\langle\tilde{v}_j(a,\mathbf{k})\,\tilde{v}^*_{j'}(a,\mathbf{k}')\rangle = \delta_{\mathrm{D}}(\mathbf{k}-\mathbf{k}')\sum_j k_j^2\,\langle|\tilde{v}_j(a,\mathbf{k})|^2\rangle\ . \tag{8}$$

Let define as $P_v(a,k) \equiv \langle|\tilde{v}_j(a,\mathbf{k})|^2\rangle$ the power spectrum of the velocity in the given spatial direction (the velocity distribution is assumed to be isotropic). Then the power spectrum of the field $\mathbf{v}$ will be

$$P_v(a,k) = \frac{P_\theta(a,k)}{k^2}\ , \tag{9}$$

where $k^2 = |\mathbf{k}|^2$.

At large redshifts the overdensity and velocity divergence amplitudes evolve according to the linear law (Peebles 1980; Crocce and Scoccimarro 2006):

$$\tilde{\delta}(a,\mathbf{k}) = \frac{D}{D_{\mathrm{i}}}\,\tilde{\delta}(a_{\mathrm{i}},\mathbf{k}) \equiv D\tilde{\delta}_{\mathrm{L}}(\mathbf{k})\ , \tag{10}$$

$$\tilde{\theta}(a,\mathbf{k}) = \frac{aHfD}{a_{\mathrm{i}}H_{\mathrm{i}}f_{\mathrm{i}}D_{\mathrm{i}}}\,\tilde{\theta}(a_{\mathrm{i}},\mathbf{k}) \equiv aHfD\tilde{\theta}_{\mathrm{L}}(\mathbf{k})\ , \tag{11}$$

where $H = H(a)$ is the Hubble parameter, $D = D(a)$ is the linear growth factor, $f \equiv d\ln D/d\ln a$, index „i“ marks the initial time. Hereinafter, by the index „L“ we will denote the values reduced to the unit growth factor, i.e. not depending on the redshift. For linear approximation for the amplitudes, the variances are subject to the quadratic growth law:

$$S(a,m) = D^2 S_{\mathrm{L}}(m) \tag{12}$$

$$S_v(a,m) = D_v^2 S_{v,\mathrm{L}}(m)\ , \tag{13}$$

where $D_v \equiv aHfD$. Physically, interesting is the situation when the initial overdensity and velocity divergence perturbations are proportional to each other. It can be shown (Crocce and Scoccimarro 2006) that in this case

$$\tilde{\delta}(a_{\mathrm{i}},\mathbf{k}) = -\frac{\tilde{\theta}(a_{\mathrm{i}},\mathbf{k})}{a_{\mathrm{i}}H_{\mathrm{i}}f_{\mathrm{i}}}\ , \tag{14}$$

i. e., the power spectra of the fields $\tilde{\delta}_{\mathrm{L}}(\mathbf{k})$ and $\tilde{\theta}_{\mathrm{L}}(\mathbf{k})$ coincide.

Due to the momentum conservation, the forming halo as a whole inherits the velocity of the proto-halo matter, namely, velocity, averaged over proto-halo mass scale

$$\mathbf{v}(a,\mathbf{x},m) = \int d^3x'\,W(\mathbf{x}'-\mathbf{x},m)\,\mathbf{v}(a,\mathbf{x}')\ . \tag{15}$$

Let assume, that a proto-halo with mass M had velocity $\mathbf{V}(a,\mathbf{X},M)$. Then the variance of a particular spatial component of the velocity $v_j(a,\mathbf{x},m)$ of a sub-halo with the mass m, to the first

approximation will depend neither on position of the sub-halo inside the proto-halo nor the velocity of the proto-halo, but only on the variance of the velocity field on the scale M[2]:

$$S_v(a, m, M) \equiv D_v^2 \left[S_{v,\mathrm{L}}(m) - S_{v,\mathrm{L}}(M) \right] . \tag{16}$$

In the present paper the ΛCDM model parameters obtained by the Planck mission Planck Collaboration et al. (2013) were adopted: $h = 0.673$, $\Omega_{\mathrm{m},0} = 0.315$, $\Omega_{\Lambda,0} = 1 - \Omega_{\mathrm{m},0} = 0.685$, $\sigma_8 = 0.828$, $n_{\mathrm{S}} = 0.9603$. The power spectrum of the overdensity fluctuations was calculated for these parameters by means of the code CAMB (Lewis et al. 2000) for wavenumbers from 10^{-3} Mpc^{-1} to 2 Mpc^{-1} (on-line interface to the CAMB is presented in the LAMBDA project 2013). Outside of this range, the theoretical power spectrum was used with the power index n_{S} and the transfer function (Bardeen et al. 1986, p. 60) with the shape parameter $\Gamma \equiv h^2 \Omega_{\mathrm{m},0} = 0.14$ Mpc^{-1}. Plots of the overdensity and velocity variances calculated in such a model are shown in the Fig. 1. The linear growth factor was adopted from Bildhauer et al. (1992) using normalization $D(a \approx 0) = a$.

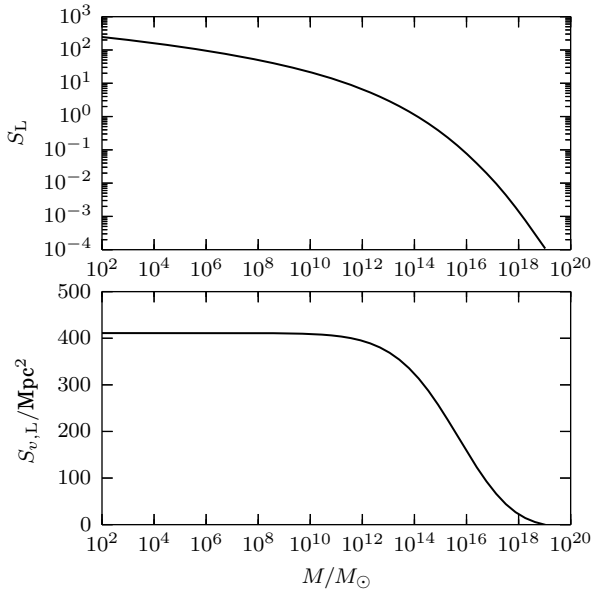

Fig. 1.— Dependence of the variance of overdensity fluctuations (upper panel) and the variance of velocity fluctuations (lower panel) on the mass scale.

[2]Closer the centers of the volumes M and m are to each other, the better this approximation is (Hoffman and Ribak 1991). See also (Kurbatov 2014).

2.2. Evolution of the mass function

The EPS model (Peacock and Heavens 1990; Bond et al. 1991) can be formulated with the excursion set approach as follows. Consider the overdensity fluctuations field $\delta(a, \mathbf{x}, m)$ with the mass scale m. If the perturbation is spherical, it can be argued that its amplitude on the linear stage is determined by the initial amplitude only (Peebles 1980), or, equivalently, by $\delta_{\rm L}(\mathbf{x}, m)$. This feature can be used to choose such perturbations which collapse and virialize to the halo stage by a given redshift. It's necessary to note, however, that some already virialized halos may be absorbed by more massive ones. Therefore, the only initial perturbations accounted in the mass function for certain redshift should be the most massive ones with required virialization time.

These ideas may be represented as a typical problem of theory of the stochastic processes. A stochastic process[3] $\delta(S)$ starts from the point $\delta = 0$ with the parameter $S = 0$, which corresponds to $m = \infty$. Its evolution obeys equation

$$\frac{d\delta}{dS} = \eta \,, \tag{17}$$

where $\eta = \eta(S)$ is a Gaussian random process with zero mean, unit variance, and the correlation function $\langle \eta(S)\, \eta(S') \rangle = \delta_{\rm D}(S - S')$ (Maggiore and Riotto 2010a). The mass m corresponding to the value of the parameter S, when a certain threshold $\delta_{\rm c}/D(z)$ is reached by the process $\delta(S)$ for the first „time“ S, is interpreted as the mass of the halo virialized by the given redshift z. The distribution function of these masses is the halo mass function sought for.

The value $\delta_{\rm c}$ is the linear amplitude of the spherical overdensity perturbation (10) collapsing at the moment z. In the spherical collapse model (Peebles 1980) this value reduced to the unit growth factor is approximately 1.686. In our case[4]

$$\delta_{\rm c} = 1.686\, D(z = 0) \,. \tag{18}$$

The resulting halo mass function can be represented as a probability density (Bond et al. 1991; Lacey and Cole 1993)

$$f^{(0)}(z, S) = \frac{\omega}{\sqrt{2\pi S^3}} \, \exp\left(-\frac{\omega^2}{2S}\right) \tag{19}$$

or the cumulative distribution function

$$F^{(0)}(z, < S) = \int_0^S dS' \, f^{(0)}(z, S') = \mathrm{erfc}\left(\frac{\omega}{\sqrt{2S}}\right) \,, \tag{20}$$

where notation $\omega \equiv \delta_{\rm c}/D(z)$ is introduced.

---

[3]Hereafter the index „L“ will be omitted as the redshift dependency will be denoted explicitly.

[4]In models of the EPS class the linear growth factor D is usually normalized to take unit value at $z = 0$ (Lacey and Cole 1993). In the present paper the alternative normalization is used: $D(z) \approx 1/(z+1)$ at $z \gg 1$. For cosmological parameters adopted here (see previous Sec.) we have $D(z = 0) \approx 0.788$.

The variance S or the mass of a halo with a largest formation rate at the given redshift correspond to the maximum of the function $\partial f^{(0)}/\partial\omega$ and thus obeys equation $\omega^2 = (3+\sqrt{6})\,S$. Most of the halos formed per unit time has the variance in the interval $\log S = \log[\omega^2/(3+\sqrt{6})]\pm 0.5$. At large redshifts, the interval can be estimated as

$$S \approx (0.15 \ldots 1.5)\,(z+1)^2\ . \tag{21}$$

It should be noted that the process $\delta(S)$ defined by Eq. (1) for an arbitrary filter strictly speaking does not comply to Eq. (17) where the r.h.s. is delta-correlated. That is, the process is not Markovian. Moreover, the spherical collapse model is quite a rough approximation, neither any possible deviations from the spherical symmetry in the initial conditions nor tidal action of environment are considered. These issues can be resolved by corrections to the excursion set formalism (Bond et al. 1991; Maggiore and Riotto 2010a,b). However in the present paper we base on the simple case of the excursion set theory.

3. Kinematic effects in the dark matter

3.1. Formation of a single halo

Transition of a spherical perturbation into a halo proceeds in four stages: initial expansion, detachment from the Hubble flow, compression, virialization (Peebles 1980). The moment of detachment or turnaround point is located approximately in the middle between the start of the expansion and the virialization, when the formation is completed (Peebles 1980). In the spherical collapse model, the halo formation is described by motion of disjoint layers or test particles in the gravitational field of a point mass. At that, the mass enclosed inside the layer is conserved. For the perturbation to become collapsed at a given redshift $z_{\rm f}$, its linear overdensity must grow as (Lacey and Cole 1993)

$$\Delta(z) = \frac{D(z)}{D(z_{\rm f})}\,\frac{\delta_{\rm c}}{D(z=0)}\ . \tag{22}$$

It was mentioned above that sub-halos have random velocities relatively to the parent halo. Let consider the possibility that the velocity of the sub-halo is large enough to leave the proto-halo. Let's write an expression for mechanical energy of a test particle inside the parent proto-halo using physical coordinates, and neglecting the Λ-term:

$$E = \frac{\dot{\mathbf{r}}^2}{2} + \Phi\ . \tag{23}$$

At large redshifts, the overdensity amplitude of the parent proto-halo is low, thus the density distribution inside the parent proto-halo may be considered as uniform. Gravitational potential in this case is

$$\Phi = -\frac{GM}{R}\left(\frac{3}{2} - \frac{r^2}{2R^2}\right)\ , \tag{24}$$

where M is the proto-halo mass; the scale R is defined as a physical radius of the proto-halo at the turnaround, containing the mass M:

$$M = \frac{4\pi}{3}\,\rho_{\mathrm{cr},0}\Omega_{\mathrm{m},0}\,(1+\Delta)\,\frac{R^3}{a^3}\ . \tag{25}$$

We formulate escape condition for the particle as the constraints for the energy value, $E > 0$:

$$(a\dot{x} + aHx)^2 > \frac{H_0^2\Omega_{\mathrm{m},0}}{a}X^2\,(1+\Delta)\left(\frac{3}{2} - \frac{x^2}{2X^2}\right)\ , \tag{26}$$

where $X = R/a$, $x = r/a$, $x \leqslant X$, $a < a_{\mathrm{f}}$. Condition (26) defines the lower bound of the velocity sufficient to leave the proto-halo:

$$\dot{x} > -Hx + \left[\frac{H_0^2\Omega_{\mathrm{m},0}}{a^3}\,X^2\,(1+\Delta)\left(\frac{3}{2} - \frac{x^2}{2X^2}\right)\right]^{1/2}\ . \tag{27}$$

Let's estimate the escape probability. Assume the following: (i) the test particle's location is near the edge of the proto-halo; (ii) the proto-halo collapses at a high redshift ($H \approx H_0\Omega_{\mathrm{m},0}^{1/2}a^{-3/2}$); (iii) the amplitude of the proto-halo is low ($\Delta \ll 1$). Then the escape condition (27) takes the form

$$\dot{x} > \frac{1}{2}\,HX\Delta\ . \tag{28}$$

Sub-halos served as the test particles in our formulation of the problem. Let's multiply the last inequality by the scale factor a, then substitute into the l.h.s. the most probable value of the relative velocity modulus of the sub-halo inside the proto-halo, assuming the Gaussian distribution with zero mean and the variance (16). Also, let express X via the proto-halo mass. In the high-z limit, the condition (27) takes the form

$$[S_v(m) - S_v(M)]^{1/2} \gtrsim 3\,(z_{\mathrm{f}}+1)\left(\frac{M}{10^{14}M_\odot}\right)^{1/3}\ \mathrm{Mpc}\ . \tag{29}$$

It can be shown (see Appendix) that in not very strict conditions ($m \to 0$, $M < 10^{14}M_\odot$) the l.h.s. of the last inequality can be estimated as

$$[S_v(0) - S_v(M)]^{1/2} \approx 1.75\,\{\dots\}\left(\frac{M}{10^{14}M_\odot}\right)^{1/3}\ \mathrm{Mpc}\ , \tag{30}$$

where expression in braces is slowly changing decreasing function of M (it becomes close to 200 when $M = 10^2M_\odot$, and 1 when $M = 10^{14}M_\odot$). Adopting (29), we get (27) in the form

$$\{\dots\} \gtrsim z_{\mathrm{f}} + 1\ . \tag{31}$$

This inequality formally shows that for any z_{f} there are perturbations which masses are small enough to obey the escape condition for its sub-halos. It is necessary to remember, however, that for any redshift there is a certain mass interval in which most of the halos form, see Eq. (21). For sub-halos

escape to have an effect upon the population formation process, the proto-halo mass must satisfy both Eqs. (21) and (29). This requirement can be represented as

$$\frac{S_v(0) - S_v(M)}{(M/10^{14} M_\odot)^{2/3}\ \mathrm{Mpc}^2} \gtrsim S(M)\ . \tag{32}$$

Let's estimate both sides of this inequality in the low-mass limit. For simplicity let use the „k-sharp" filter for which the Fourier image is $\tilde{W}(\mathbf{k}, M) = \theta(1 - kX)$. Then the overdensity and the velocity variances are

$$S(M) \propto \int_0^{X^{-1}(M)} dk\, k^2 P(k) \tag{33}$$

and

$$S_v(0) - S_v(M) \propto \int_{X^{-1}(M)}^{\infty} dk\, P(k)\ . \tag{34}$$

Calculating the differentials, it's easy to show that

$$\frac{d}{dS}\frac{S_v(0) - S_v(M)}{M^{2/3}} \propto -1 + \frac{2X}{P(X^{-1})}\int_{X^{-1}}^{\infty} dk\, P(k)\ , \tag{35}$$

where the proportionality factor is a positive constant. We assumed also $k \equiv X^{-1}$. Defining the power spectrum as $P(k) \equiv \Pi(k)/k^3$, by formal integration of the r.h.s we obtain

$$\frac{d}{dS}\frac{S_v(0) - S_v(M)}{M^{2/3}} \propto \frac{1}{X^2 \Pi(X^{-1})}\int d\Pi'\, X'^2 \geqslant 0\ . \tag{36}$$

If Π is a constant (this is true in a rough approximation) then the r.h.s. of (36) is zero. In a more strict approximation we have $\Pi \propto \ln^2(k/\Gamma)$ i.e. slowly growing function of the wavenumber (Bardeen et al. 1986). The conclusion is: the lesser proto-halo mass is, the lesser the probability for its sub-halos to escape. Given that the formation of the structures with time goes from the low masses to the larger ones, it can be argued that in the high redshift limit the sub-halo escape does not affect the formation of the dark halo population.

Let's denote as $\sigma_v \equiv [S_v(m) - S_v(M)]^{1/2}$ the standard deviation of the 1-D velocity (reduced to the unit growth factor) of a sub-halo m relatively to a proto-halo M. The probability for modulus of the Gaussian distributed sub-halo velocity to exceed some v is

$$P_v(> v) = \mathrm{erfc}\left(\frac{v}{\sqrt{2}\,\sigma_v}\right) + \frac{2}{\sqrt{\pi}}\,\frac{v}{\sqrt{2}\,\sigma_v}\,\exp\left(-\frac{v^2}{2\sigma_v^2}\right)\ . \tag{37}$$

Given the uniform spatial distribution of the sub-halos at the early stage of the proto-halo evolution, the probability for sub-halo m to escape proto-halo M formed at the redshift z_f is

$$\chi_\mathrm{ej}(z_\mathrm{f}, M, m) \equiv \frac{3}{X^3}\int_0^X dx\, x^2 P_v(> v_\mathrm{ej})\ , \tag{38}$$

where a threshold velocity value v_ej is the r.h.s. of (27) reduced to the unit growth factor:

$$v_\mathrm{ej} = -\frac{aH}{D_v}\,x + \left[\frac{H_0^2 \Omega_{\mathrm{m},0}}{aD_v^2}\,X^2\,(1+\Delta)\left(\frac{3}{2} - \frac{x^2}{2X^2}\right)\right]^{1/2}\ . \tag{39}$$

Distribution of $\chi_{\rm ej}$ for the sub-halos of low masses is shown in Fig. 2. Comparing the position of contour lines and the mass interval of proto-halos formed by a given era (the mass interval is bounded by thick dashed lines), one can see that for the formation redshifts $z_{\rm f} \lesssim 100$ the mass fraction of escaping sub-halos of low masses is approximately constant for all $z_{\rm f}$ and can be estimated as 30%, roughly. The same is true in the case when the sub-halo mass is one-third of that of the proto-halo, but the escaping mass fraction is about 15% (see Fig. 3). Thereby, a significant fraction of the sub-halos can escape the parent proto-halo, thus avoiding the absorption.

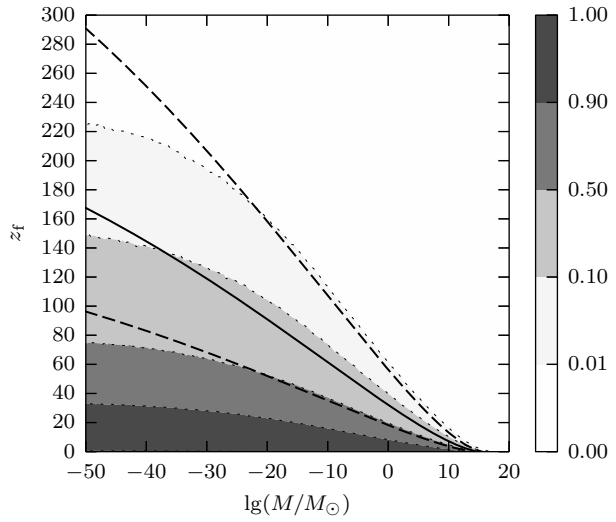

Fig. 2.— Isolines of the probability of ejection of sub-halos as a function of proto-halo mass (horizontal axis) and redshift (vertical axis). The probability is estimated using Eq. (29) for sub-halo masses $m \to 0$. The solid curve marks the era of the most intensive formation proto-halo of a given mass. The primary mass interval of the proto-halos formed at a given epoch is bounded by the dashed lines.

3.2. Evolution of the mass function with account for kinematic effects

In the standard excursion set approach a mass inside each collapsed perturbation is conserved during the collapse and equals to the subsequent halo mass. This suggestion makes realizations of the random process $\delta(S)$ independent up to some small corrections noted above. As it became clear, proto-halos may loss a significant fraction of the sub-halos resulting in transition of the sub-halos to proto-halo of larger scales which undergo collapse at later times. Consequently, the values of $\delta(S)$ will correlate both in scales and redshifts. This fact makes it difficult to use the excursion set formalism explicitly.

Greater clarity can have an approach based on the kinetic equation, when the evolution of the mass function explicitly presented as a result of the absorption process of the sub-halo by the

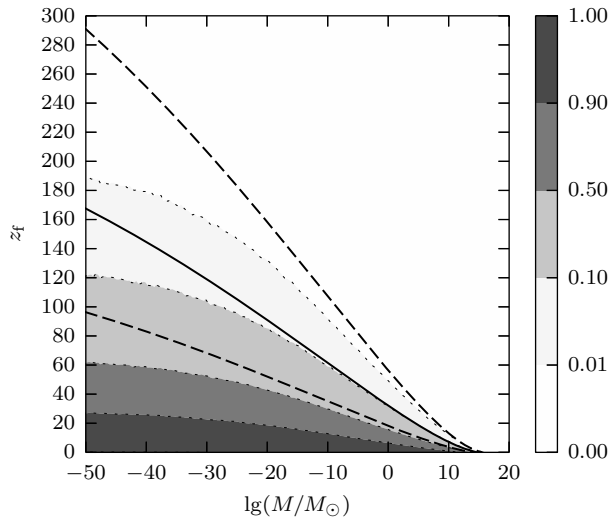

Fig. 3.— Same as in the Fig. 2, but the sub-halo masses are one-third of the proto-halo mass.

large-scale perturbations. Let's write the total probability of a halo formation at the moment ω_1, the mass of which corresponds to the interval $(S_1, S_1 + dS_1)$, and another halo $(S_2, S_2 + dS_2)$ at the moment ω_2, given conditions $S_1 > S_2$ and $\omega_1 > \omega_2$:

$$p^{(0)}(\omega_1, S_1;\, \omega_2, S_2)\, dS_1 dS_2 = f^{(0)}(\omega_1, S_1 \,|\, \omega_2, S_2)\, f^{(0)}(\omega_2, S_2)\, dS_1 dS_2 = \tag{40}$$

$$= f^{(0)}(\omega_2, S_2 \,|\, \omega_1, S_1)\, f^{(0)}(\omega_1, S_1)\, dS_1 dS_2 \;, \tag{41}$$

where $f^{(0)}(\omega, S)$ is the PS mass function (19). Reducing the total probability, one obtains

$$\int_{S_2}^{\infty} dS_1\, p^{(0)}(\omega_1, S_1;\, \omega_2, S_2) = f^{(0)}(\omega_2, S_2) \;, \tag{42}$$

$$\int_{0}^{S_1} dS_2\, p^{(0)}(\omega_1, S_1;\, \omega_2, S_2) = f^{(0)}(\omega_1, S_1) \;. \tag{43}$$

These relations suggest a possible form of the kinetic equation:

$$f^{(0)}(\omega, S) - f^{(0)}(\omega + \Delta\omega, S) = \\ = \int_{S}^{\infty} dS'\, p^{(0)}(\omega + \Delta\omega, S';\, \omega, S) - \int_{0}^{S} dS'\, p^{(0)}(\omega + \Delta\omega, S;\, \omega, S') \;, \tag{44}$$

i.e.

$$-\frac{\partial f^{(0)}(\omega, S)}{\partial \omega} = \\ = \lim_{\Delta\omega \to 0+} \frac{1}{\Delta\omega} \left[\int_{S}^{\infty} dS'\, p^{(0)}(\omega + \Delta\omega, S';\, \omega, S) - \int_{0}^{S} dS'\, p^{(0)}(\omega + \Delta\omega, S;\, \omega, S') \right] \;. \tag{45}$$

There is a „minus“ sign in the l.h.s. of Eq. (45) because the ω parameter decreases with the time. Terms in the r.h.s. are the source and the sink respectively.

According to the total probability formula (40, 41) the source and the sink can be written in different ways. We choose the way which leads to the most familiar form of kinetic equation:

$$-\frac{\partial f^{(0)}(\omega,S)}{\partial\omega} = \lim_{\Delta\omega\to 0+}\frac{1}{\Delta\omega}\Bigg[\int_S^\infty dS'\, f^{(0)}(\omega,S\,|\,\omega+\Delta\omega,S')\, f^{(0)}(\omega+\Delta\omega,S') - \tag{46}$$

$$- f^{(0)}(\omega+\Delta\omega,S)\int_0^S dS'\, f^{(0)}(\omega,S'\,|\,\omega+\Delta\omega,S)\Bigg]\,. \tag{47}$$

„Transfer cross section“ here is the conditional PDF $f^{(0)}(\omega,S\,|\,\omega+\Delta\omega,S')$, and the unknown function is $f^{(0)}(\omega+\Delta\omega,S)$. Since the random process $\delta(S)$ is considered as markovian, it can be argued (Lacey and Cole 1993) that $f^{(0)}(\omega_1,S_1\,|\,\omega_2,S_2) = f^{(0)}(\omega_1-\omega_2,S_1-S_2)$. Expression for conditional PDF $f^{(0)}(\omega_2,S_2\,|\,\omega_1,S_1)$ can be obtained via the formula of total probability (40,41).

Let's modify the source and the sink of (46) in a way to allow the mass ejection from the forming halos. Consider the probability $f^{(0)}(\omega,S\,|\,\omega+\Delta\omega,S')\,dS$, which is a mass fraction of fluctuations having variance range from S to $S+dS$ and collapsing by the time ω, after each absorbs halos S', which existed before by the time $\omega+\Delta\omega$. As the sub-halos S' may escape the proto-halo, this fraction may decrease.

Let denote as $f(\omega,S)$ the unknown mass function and to assume that the statistics of the fluctuations is not affected by the sub-halos ejection occurring in other proto-halos (those which collapsed earlier). In this case, the product $[1-\chi_{\rm ej}(\omega,S,S')]\,f^{(0)}(\omega,S\,|\,\omega+\Delta\omega,S')\,f(\omega+\Delta\omega,S')\,dS$ gives contribution to the mass of the halo S by the sub-halos S', which could not leave the parent. Then the mass fraction of all the halos that form during interval $\Delta\omega$ is

$$P_+(\omega+\Delta\omega,\omega,S)\,dS \equiv$$

$$\equiv dS\int_S^\infty dS'\,[1-\chi_{\rm ej}(\omega,S,S')]\,f^{(0)}(\omega,S\,|\,\omega+\Delta\omega,S')\,f(\omega+\Delta\omega,S')\,. \tag{48}$$

Here $f(\omega+\Delta\omega,S')$ is the mass function of the halos formed by the time $\omega+\Delta\omega$. Expression (48) is the first component of the source. It corresponds to the mass redistribution after growth and virialization of the perturbations. Besides that, we need to take into account those of the sub-halos which leave the proto-halos and return to the population:

$$P_{+,\rm re}(\omega+\Delta\omega,\omega,S) \equiv \int_0^S dS''\,\chi_{\rm ej}(\omega,S'',S)\,f^{(0)}(\omega,S''\,|\,\omega+\Delta\omega,S)\,f(\omega+\Delta\omega,S)\,. \tag{49}$$

This term must be incorporated into the source with negative sign.

The sink also has two components:

$$P_-(\omega+\Delta\omega,\omega,S) \equiv f(\omega+\Delta\omega,S)\,Q_-(\omega+\Delta\omega,\omega,S)\,, \tag{50}$$

$$P_{-,\mathrm{re}}(\omega+\Delta\omega,\omega,S) \equiv f(\omega+\Delta\omega,S)\,Q_{-,\mathrm{re}}(\omega+\Delta\omega,\omega,S)\;, \tag{51}$$

where

$$Q_{-}(\omega+\Delta\omega,\omega,S) \equiv \int_0^S dS''\,[1-\chi_{\mathrm{ej}}(\omega,S'',S)]\,f^{(0)}(\omega,S''\,|\,\omega+\Delta\omega,S)\;, \tag{52}$$

$$Q_{-,\mathrm{re}}(\omega+\Delta\omega,\omega,S) \equiv \int_0^S dS''\,\chi_{\mathrm{ej}}(\omega,S'',S)\,f^{(0)}(\omega,S''\,|\,\omega+\Delta\omega,S)\;. \tag{53}$$

After all substitutions, the kinetic equation has the form:

$$-\frac{\partial f}{\partial\omega} = \lim_{\Delta\omega\to 0+}\frac{1}{\Delta\omega}\left[P_+ - P_{+,\mathrm{re}} - (P_- - P_{-,\mathrm{re}})\right]\;. \tag{54}$$

It's easy to show by evaluation that

$$\int_0^\infty dS\,(P_+ + P_{-,\mathrm{re}}) = \int_0^\infty dS\,(P_- + P_{+,\mathrm{re}}) = 1\;. \tag{55}$$

Expressions (54) and (55) reveal that the normalization of the PDF f is conserved with the time. Note also that $P_{+,\mathrm{re}} = P_{-,\mathrm{re}}$. Let's finally rewrite the equation (54) using Taylor expansion in $\Delta\omega$ and obtain then a recurrent procedure for calculation of the mass function:

$$f(\omega,S) = f(\omega+\Delta\omega,S) + P_+(\omega+\Delta\omega,\omega,S) - f(\omega+\Delta\omega,S)\,Q_-(\omega+\Delta\omega,\omega,S) + \mathcal{O}(|\Delta\omega|^2)\;. \tag{56}$$

Neglecting the quadratic residue, the recurrent relation (56) can be written as

$$f(\omega,S) = \int_0^\infty dS'\,r(\omega,S\,|\,\omega+\Delta\omega,S')\,f(\omega+\Delta\omega,S')\;, \tag{57}$$

where

$$r(\omega,S\,|\,\omega+\Delta\omega,S') = \theta(S'-S)\,q(\omega,S\,|\,\omega+\Delta\omega,S') + \tag{58}$$

$$+\,\delta_{\mathrm{D}}(S-S') - \delta_{\mathrm{D}}(S-S')\int_0^{S'} dS''\,q(\omega,S''\,|\,\omega+\Delta\omega,S')\;, \tag{59}$$

and

$$q(\omega,S\,|\,\omega+\Delta\omega,S') \equiv [1-\chi_{\mathrm{ej}}(\omega,S,S')]\,f^{(0)}(\omega,S\,|\,\omega+\Delta\omega,S')\;. \tag{60}$$

The representation (57) is useful for numerical solution of the kinetic equation by Monte-Carlo method. One step of the solution procedure may look like this:

(a) generate the random value S' with initial PDF $f(\omega,S')$;

(b) generate the random value S according to the transition PDF (58);

(c) redefine $\omega-\Delta\omega \mapsto \omega$, $S \mapsto S'$ and go to (b).

A cumulative transfer distribution function is more convenient for this algorithm than the PDF:

$$\int_0^S dS''\, r(\omega, S'' \,|\, \omega + \Delta\omega, S') = \begin{cases} \displaystyle\int_0^S dS''\, q(\omega, S'' \,|\, \omega + \Delta\omega, S') \,, & S \leqslant S' \\ 1 \,, & S > S' \end{cases} \tag{61}$$

Examples of how the sub-halo ejection affects the halo mass function are shown in Fig. 4. In these calculations, the escape probability was assumed constant. Also the EPS mass function was used as the initial PDF. It is clearly seen that for larger escape probability $\chi_{\rm ej}$ the „tail“ of the low mass end (high S values) of the mass function becomes heavier , i.e. the evolution of the population effectively slows down as $\chi_{\rm ej}$ increases.

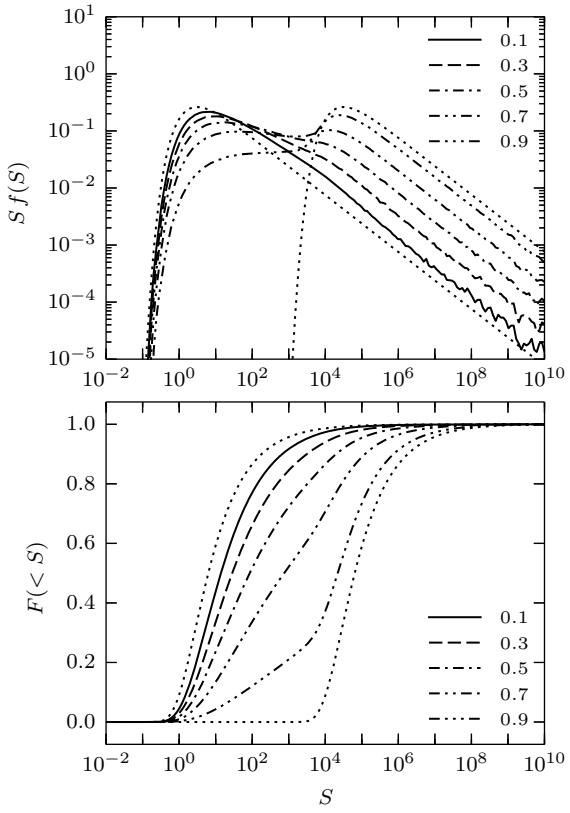

Fig. 4.— The mass function (PDF and the cumulative) for the case $\chi_{\rm ej} \equiv$ const. The rightmost dashed line designates the initial distribution at $z = 100$ for all runs. The leftmost dashed line designates the final distribution $z = 0$) for the case $\chi_{\rm ej} = 0$. The intermediate curves correspond to various $\chi_{\rm ej}$ (see the legend on the plot).

3.3. Choice of initial conditions

In the kinetic approach presented above it is possible to use an appropriate arbitrary initial mass function. Thus, the problem of the choice of the initial conditions arises. According to the modern cosmological theory, matter-dominated era started at $z \approx 3 \times 10^3$ (Gorbunov and Rubakov 2011). According to the formal relation (21), structures with the variances $S \sim 10^6 \dots 10^7$ or masses $\log(m/M_\odot) \ll -100$ formed at that era (see Appendix). It is obvious, however, that the masses of the structures can not be lower than the mass of a hypothetical dark matter particle. If we take the value $m_{\rm DM} = 100$ GeV $\sim 10^{-55} M_\odot$ as the mass of the dark matter particle (this value corresponds to $S_{\rm DM} \approx 10^4$), then the earliest structures may form at the redshifts as low as $z \sim 100$ (see Eq. (21)), and it is unlikely for structures to form at the higher redshifts. Finally, recalling the sub-halo escape model, we see that the sub-halos can not escape at the redshifts greater than 250 (see Fig. 2). Considering all these restrictions, we assume the redshift value $z_{\rm i} \equiv 300$ as the initial moment for all calculations below. As the initial mass function we assume the cumulative distribution function

$$F(\omega_{\rm i}, < S) = \begin{cases} F^{(0)}(\omega_{\rm i}, < S) \, , & S \leqslant S_{\rm DM} \\ 1 \, , & S > S_{\rm DM} \, , \end{cases} \tag{62}$$

where $\omega_{\rm i} = \delta_{\rm c}/D(z_{\rm i})$. Note that $F^{(0)}(\omega_{\rm i}, < S_{\rm DM}) \sim 10^{-7}$.

In Fig. 5 the mass functions in the model without sub-halo ejection ($\chi_{\rm ej} = 0$) are plotted for the different redshifts. The initial mass function (62) peaks at the greater masses relatively to the peak of the EPS mass function (at $z = 300$ the EPS peaks at $S \sim 10^5$), so the mass function at the subsequent times is also shifted to the higher masses. However, at $z \lesssim 15$ the massive end of the distribution coincides with the EPS model. In general, the low mass end of the mass function is suppressed at all redshifts, because of absence of the structures of mass $m_{\rm DM}$ and lower.

Obvious consequence of using the initial mass function suggested in this section is that the formation of the structures with masses lower than $m_{\rm DM}$ is impossible. This property may be used for the analysis of the resolution effects of cosmological codes built on top of the N-body or grid methods. The lowest possible mass scale in such applications should correspond to the spatial resolution of the numerical method.

3.4. Account for the background structure

Effect of the low density background structure (the supercluster or the void) can be considered in our model. Such a structure may be set in terms of the statistical constraints for the field of the overdensity fluctuations (Kurbatov 2014). Applying the constraints leads to considerable change in statistics of modes of the fluctuations. E.g. the statistics is not more spatially uniform, the perturbations field „feels“ the size and shape of the background structure. Thus, the halo mass function also changes. In the EPS theory the effects of the background was considered first by Bond et al. (1991); Bower (1991), and investigated further by Mo and White (1996); Sheth and Tormen (1999)

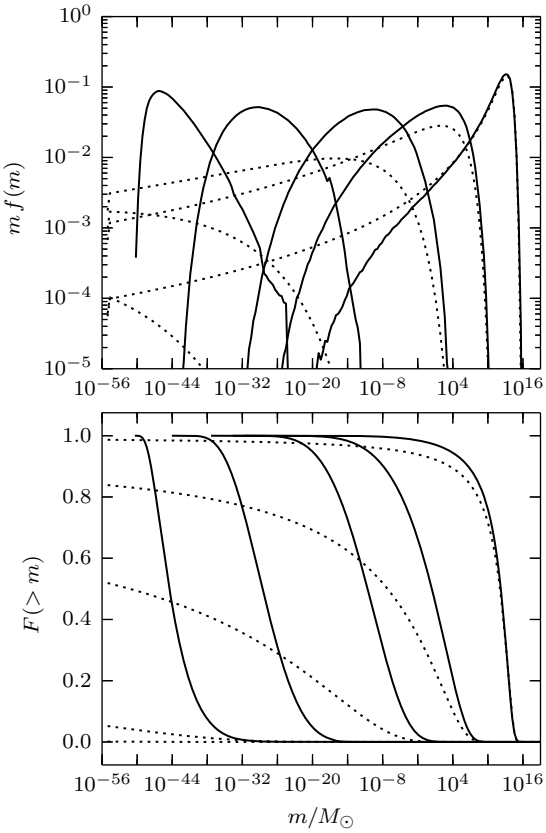

Fig. 5.— Mass function (PDF and the cumulative) for the case $\chi_{\rm ej} = 0$ and the initial conditions Eq. (62). The dotted lines designates the PS mass functions. Five epochs are represented in the plot (from left to right on both panels): $z = 250$, $z = 150$, $z = 50$, $z = 15$, and $z = 0$.

and others. When deviation of density of the background structure from uniform distribution is low, and the structure is large enough in all directions, the effect of the background presence can be accounted by a simple approach. Let's denote $S_{\rm B} \equiv S(m_{\rm B})$ the variance of the overdensity fluctuations averaged over the background structure's mass scale $m_{\rm B}$, then the variance of the field over the mass scale $m \ll m_{\rm B}$ placed deep inside the background structure is approximately $S(m) - S_{\rm B}$ (Hoffman and Ribak 1991; Kurbatov 2014). The same considerations are true for the velocity fluctuations field also (this fact was already utilized when the escape criterion (16) was obtained).

Bond et al. (1991); Bower (1991) have shown that the large scale background structure can be easily applied to the PS mass function Eq. (19) by formal substitutions of the kind

$$\omega \mapsto \omega - \omega_{\rm B}\ , \qquad S \mapsto S - S_{\rm B}, \tag{63}$$

where $\omega_{\rm B}$ is the background overdensity calculated via the linear law (10), and reduced to the unit growth factor:

$$\omega_{\rm B} = \frac{D(z=0)}{D(z_{\rm i})}\,\Delta(z_{\rm i}) = \frac{\delta_{\rm c}}{D(z_{\rm f})}\ . \tag{64}$$

The second equality in this expression allows to define an overdense structure which collapses by the moment $z_{\rm f}$. The equivalent description can be reached in the kinetic approach proposed in the previous section, if the substitutions (63) are made in the transfer PDF $f^{(0)}(\omega, S\,|\,\omega+\Delta\omega, S')$.

The same substitutions may be utilized in the model with kinematic effects. It should be noted however, that the substitutions (63) must not be applied to escape probability $\chi_{\rm ej}(\omega, S, S')$, because in fact the probability depends on the redshift and the halo mass, but not the overdensity threshold and the overdensity variance. Moreover, the velocity variance already enters Eq. (38), as the difference, hence its value, does not change as the velocity field varies, if these changes have the form (63). Finally, the transfer cross section is

$$q(\omega, S\,|\,\omega+\Delta\omega, S') = [1-\chi_{\rm ej}(\omega, S, S')]\,f^{(0)}(\omega-\omega_{\rm B}, S-S_{\rm B}\,|\,\omega-\omega_{\rm B}+\Delta\omega, S'-S_{\rm B})\ , \tag{65}$$

where $\omega_{\rm B} \equiv \delta_{\rm B}/D$. Note that the initial conditions (62) must not be transformed by (63).

4. Virialized matter in the local Universe

Mass counts of the galaxies, virialized groups of galaxies, and clusters, made by many authors reveal the deficiency of the mass inside virialized objects, up to the factor three (see references in Makarov and Karachentsev (2011)) compared to predictions of ΛCDM model. According to the catalog Makarov and Karachentsev (2011), local density parameter of the matter

$$\Omega_{\rm m} \equiv \frac{3M_{\rm m,tot}}{4\pi\rho_{\rm cr,0}D^3}\ , \tag{66}$$

may be estimated as 0.08 ± 0.02. Here $M_{\rm m,tot}$ is the total mass of the matter inside a sphere of radius D. The authors of the catalog proposed several explanations of the deficiency. The most plausible of them is the suggestion about possibility that the essential part of the dark matter in the Universe (about 2/3) is scattered outside the virial or collapsing regions, being distributed diffusively or concentrated in dark „clumps“ (Makarov and Karachentsev 2011). Certain evidence for existence of the dark clumps may be provided by the observations of weak lensing events (Natarajan and Springel 2004; Jee et al. 2005), and the properties of the disturbed dwarf galaxies (Karachentsev et al. 2006).

The estimate $\Omega_{\rm m} = 0.08 \pm 0.02$ was obtained by Makarov and Karachentsev (2011) using the total mass of all virialized groups of galaxies having velocities up to 3500 km/s. To estimate the distances and masses the authors used Hubble parameter's value 73 km/s Mpc. Thus the distance D can be estimated as $3500/73 \approx 48$ Mpc, and the estimate of the total mass of the matter (given $\Omega_{\rm m,0} = 0.28$) is $1.92\times10^{16}M_\odot$. The value of the Hubble parameter adopted in the present paper is $H_0 = 67.3$ km/s Mpc, whence $D = 52$ Mpc, and the total mass is thus $M_{\rm m,tot} \approx 2.33\times10^{16}M_\odot$.

The variation of the Hubble parameter causes just a minor correction to the estimated galactic masses, about 8%. The estimate of the local matter density parameter changes more significantly and gives (when the masses of galaxies are corrected also) $\Omega_{\rm m} = 0.068 \pm 0.017 = (0.22 \pm 0.05)\Omega_{\rm m,0}$. The claims of Makarov and Karachentsev (2011) were based on observational data of the virialized groups having masses above $\approx 3 \times 10^{10} M_\odot$, and containing at least two galaxies. Completeness of the sample was 82%. The mass distribution function of the virialized groups (see Fig. 8 in Makarov and Karachentsev (2011)) showed decrease of the number of objects with masses lower than $10^{13} M_\odot$. This can be caused by the absence of the field galaxies in the sample. In the further analysis we will use just a fraction of the sample composed by the objects as massive as $10^{13} M_\odot$ and above. The reason is that this fraction should more closely match the mass distribution of the dark matter gravitational condensations.

According to EPS distribution, the total mass fraction of the dark matter halos more massive than $10^{13} M_\odot$ is $M_{\rm m}(> 10^{13} M_\odot)/M_{\rm m,tot} \approx 0.27$, i.e. more than 2/3 of all the dark matter settles in the halos with masses below $10^{13} M_\odot$ (see Fig. 6). Calculation of the model presented in Section 3.2, performed neglecting the sub-halo escape but using the initial conditions (62) leads to approximately the same distribution as the EPS predicts (dashed line on Fig. 6). The observational data (thick solid line on Fig. 6) show the deficit of the virialized halos, up to the factor two and a half comparing to the EPS prediction: $M_{\rm m}(> 10^{13} M_\odot)/M_{\rm m,tot} \approx 0.11$.

Accounting for the effect of sub-halos escape in the presented model, gives the cumulative fraction of all the massive halos about 0.08, i.e. slightly lower than observed. The most part of the matter is not incorporated into the structures as massive as $10^{13} M_\odot$ and above but becomes distributed nearly uniformly in structures with masses greater than $10^{-10} M_\odot$ (see Fig. 7). Quite a good agreement between the observed and the theoretical distribution functions of the massive halos is mainly due to the fact that the differential distribution functions for both cases nearly coincide at the masses from $3 \times 10^{13} M_\odot$ and above (see the upper plot in Fig. 6), whereas two left bins on this plot show twice as large deficit of the halos predicted the theoretical model suggested in this study. While the uncertainties in the estimates of the groups' masses can be as high as 20% (Makarov and Karachentsev 2011), the average values of the observed mass function are systematically higher than those of the theoretical one. This may be explained in two ways:

(i) Average matter density in the vicinities of the local Supercluster seems to be higher than cosmological value (Makarov and Karachentsev 2011). As a consequence of this, the massive tail of the halo mass PDF should be heavier (Mo and White 1996; Kurbatov 2014).

(ii) The proposed effect of the mass decrease of proto-halos may be overestimated as we did not account for, e.g., accretion of the matter on the proto-halo from its environment. Diemand et al. (2007) have shown that halo may accrete up to 20% of mass after virialization has ended, i,e., accretion may partially compensate the escape process leading to effective decrease of the escape probability $\chi_{\rm ej}$.

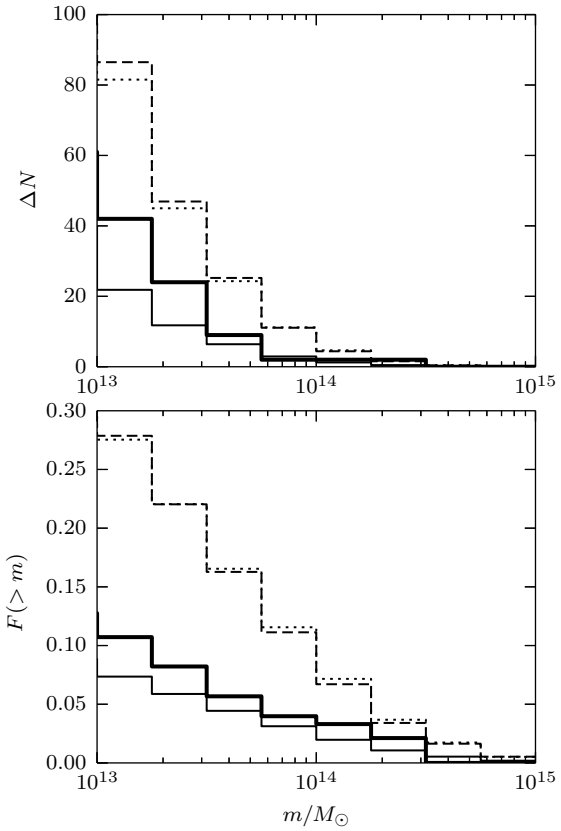

Fig. 6.— Mass function of the virialized structures with masses $> 10^{13} M_\odot$: tMakarov and Karachentsev (2011) (thick solid line), the model with sub-halo ejection (thin solid line), the model without ejection, but with the initial conditions Eq. (62) (dashed line), the PS model (dotted line).

In general, a good agreement between the observed mass function (Makarov and Karachentsev 2011) and predictions of the model proposed in this paper should be noted.

5. Conclusions

In the present paper the influence of the dark matter random velocities on formation of the dark halos population is considered. It is shown that this kinematic effect leads to the escape of the significant fraction of sub-halos (up to 30%). However, at the redshifts greater than 250 the escape is negligible. At the moderate and small redshifts the escape probability is higher for sub-halos of lower masses.

We suggested a model of the dark halo population formation, based on the EPS theory. The model was built in the frame of kinetic approach where the source and the sink explicitly describe

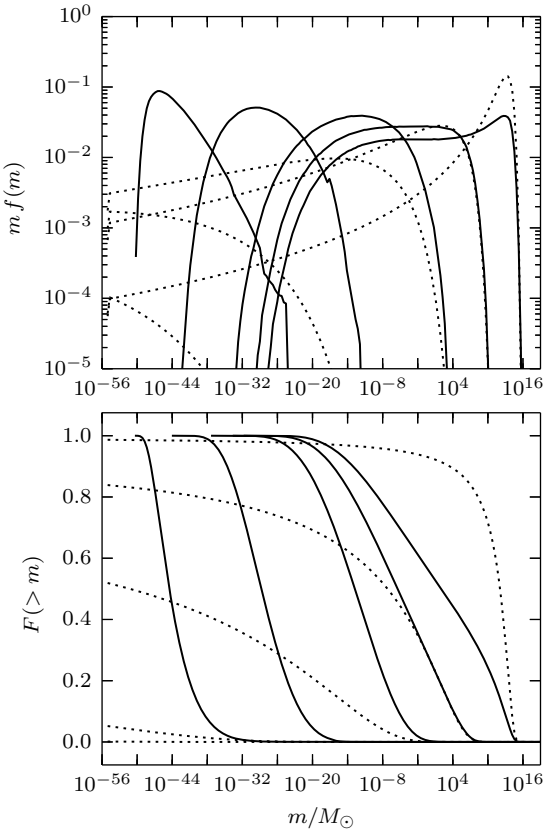

Fig. 7.— Mass function (PDF and the cumulative) calculated with Eq. (38). Lines indicate the same as in Fig. 5.

the hierarchical merging process and the kinematic effects, and potentially may be used to account environmental effects. Special initial conditions were proposed to use with the kinetic equation where the lowest possible halo mass exists corresponding to the dark halo particle's mass. The consequences of these initial conditions are systematic shift of the low-mass end of the mass distribution function towards high masses. However, this shift is almost invisible in the high-mass end at lower redshifts. The consequences of the sub-halo escape is the redistribution of the massive halos toward lower masses. If no escape is included, the EPS mass function is the invariant solution of the kinetic equation.

The model developed in this paper allowed to explain quantitatively the observable deficit of the virialized objects in the Local Universe, at least for groups of galaxies with masses greater than $10^{13} M_\odot$. The missing matter is distributed over the low-mass halos down to the lowest limit.

We need to note that the kinetic approach proposed in this paper, with the initial conditions limiting the lowest possible halo mass, may be used for analysis of the resolution effects in the cosmological numerical codes.

6. Appendix A

Let us obtain an approximate expression for the overdensity variance reduced to unity scale factor:

$$S(M) = \int d^3k\, |\tilde{W}(\mathbf{k}, M)|^2\, P(k)\ . \tag{67}$$

Assume „k-sharp“ filter with the Fourier image $\tilde{W}(\mathbf{k}, M) = \theta(1-kX)$, where $X = (3M/4\pi\Omega_{\rm m,0}\rho_{\rm cr,0})^{1/3}$. Then the variance is

$$S(M) = \frac{1}{2\pi^2} \int_0^{X_M^{-1}} dk\, k^2 P(k)\ . \tag{68}$$

The overdensity power spectrum for large wavenumbers may be written as (Bardeen et al. 1986)

$$P \approx Ak^{n_{\rm S}}\, \frac{\ln^2(2.34k/\Gamma)}{k^4}\ , \tag{69}$$

where constant A is defined by normalization σ_8; $\Gamma = h^2\Omega_{\rm m,0}$ Mpc^{-1}. Assume $M \ll M_*$, then

$$S(M) \approx S(M_*) + \frac{A}{2\pi^2(1-n_{\rm S})^3\Gamma^{1-n_{\rm S}}} \left[\frac{(1-n_{\rm S})^2 \ln^2 \varkappa + 2(1-n_{\rm S})\ln\varkappa + 2}{\varkappa^{1-n_{\rm S}}}\right]_{(\Gamma X)^{-1}}^{(\Gamma X_*)^{-1}}\ . \tag{70}$$

Making all substitutions, we obtain

$$S(M) \approx 1.29 + 10^4 \left[2.052 - \left(0.001 \lg^2 M_{14} - 0.062 \lg M_{14} + 2\right) M_{14}^{0.01323}\right]\ , \tag{71}$$

where $M_{14} \equiv M/10^{14} M_\odot$.

The variance of the relative velocity of a low mass sub-halo inside the parent halo can be estimated in a similar way. The variance on a mass scale M reduced to the unit growth factor is

$$S_v(M) = \int d^3k\, |\tilde{W}(\mathbf{k}, M)|^2\, \frac{P(k)}{k^2} = S_v(0) - \frac{1}{2\pi^2} \int_{X^{-1}}^{\infty} dk\, P(k)\ . \tag{72}$$

The relative velocity variance for low-mass sub-halos is then

$$S_v(0) - S_v(M) \approx \frac{A}{2\pi^2\Gamma^{3-n_{\rm S}}}\, \frac{(3-n_{\rm S})^2 \ln^2\varkappa + 2(3-n_{\rm S})\ln\varkappa + 2}{(3-n_{\rm S})^3 \varkappa^{3-n_{\rm S}}}\bigg|_{\varkappa=(\Gamma X)^{-1}}\ . \tag{73}$$

Assuming that the power spectrum has unit spectral index $n_{\rm S} = 1$, after all substitutions we have:

$$[S_v(0) - S_v(M)]^{1/2} \approx 1.75 \left[1.178 \log^2 M_{14} - 3.55 \log M_{14} + 3.17\right]^{1/2} M_{14}^{1/3}\ , \tag{74}$$

The expression in the square root term is a slowly changing monotonic decreasing function of the proto-halo mass. Approximately, it is 14 for $M = 10^2 M_\odot$ and unity for $M = 10^{14} M_\odot$.

REFERENCES

LAMBDA – Legacy Archive for Microwave Background Data Analysis, 2013. URL http://lambda.gsfc.nasa.gov/.

J. M. Bardeen, J. R. Bond, N. Kaiser, and A. S. Szalay. The statistics of peaks of Gaussian random fields. *ApJ*, 304:15–61, May 1986. doi: 10.1086/164143.

S. Bildhauer, T. Buchert, and M. Kasai. Solutions in Newtonian cosmology - The pancake theory with cosmological constant. *A&A*, 263:23–29, September 1992.

J. R. Bond, S. Cole, G. Efstathiou, and N. Kaiser. Excursion set mass functions for hierarchical Gaussian fluctuations. *ApJ*, 379:440–460, October 1991. doi: 10.1086/170520.

R. G. Bower. The evolution of groups of galaxies in the Press-Schechter formalism. *MNRAS*, 248: 332–352, January 1991.

M. Crocce and R. Scoccimarro. Renormalized cosmological perturbation theory. *Phys. Rev. D*, 73 (6):063519–+, March 2006. doi: 10.1103/PhysRevD.73.063519.

J. Diemand, M. Kuhlen, and P. Madau. Formation and Evolution of Galaxy Dark Matter Halos and Their Substructure. *ApJ*, 667:859–877, October 2007. doi: 10.1086/520573.

D. S. Gorbunov and V. A. Rubakov. *Introduction to the Theory of the Early Universe: Hot Big Bang Theory*. World Scientific Publishing Co. Pte. Ltd., 5 Toh Tuck Link, Singapore 596224, 2011.

Y. Hoffman and E. Ribak. Constrained realizations of Gaussian fields - A simple algorithm. *ApJ*, 380:L5–L8, October 1991. doi: 10.1086/186160.

M. J. Jee, R. L. White, N. Benítez, H. C. Ford, J. P. Blakeslee, P. Rosati, R. Demarco, and G. D. Illingworth. Weak-Lensing Analysis of the z˜=0.8 Cluster CL 0152-1357 with the Advanced Camera for Surveys. *ApJ*, 618:46–67, January 2005. doi: 10.1086/425912.

I. D. Karachentsev, V. E. Karachentseva, and W. K. Huchtmeier. Disturbed isolated galaxies: indicators of a dark galaxy population? *A&A*, 451:817–820, June 2006. doi: 10.1051/0004-6361:20054497.

E. P. Kurbatov. The mass function of dark halos in superclusters and voids. *Astronomy Reports*, 58:386–398, June 2014. doi: 10.1134/S1063772914060031.

C. Lacey and S. Cole. Merger rates in hierarchical models of galaxy formation. *MNRAS*, 262: 627–649, June 1993.

A. Lewis, A. Challinor, and A. Lasenby. Efficient Computation of Cosmic Microwave Background Anisotropies in Closed Friedmann-Robertson-Walker Models. *ApJ*, 538:473–476, August 2000. doi: 10.1086/309179.

M. Maggiore and A. Riotto. The Halo Mass Function from Excursion Set Theory. I. Gaussian Fluctuations with Non-Markovian Dependence on the Smoothing Scale. *ApJ*, 711:907–927, March 2010a. doi: 10.1088/0004-637X/711/2/907.

M. Maggiore and A. Riotto. The Halo mass function from Excursion Set Theory. II. The Diffusing Barrier. *ApJ*, 717:515–525, July 2010b. doi: 10.1088/0004-637X/717/1/515.

D. Makarov and I. Karachentsev. Galaxy groups and clouds in the local ($z\tilde{0}.01$) Universe. *MNRAS*, 412:2498–2520, April 2011. doi: 10.1111/j.1365-2966.2010.18071.x.

H. J. Mo and S. D. M. White. An analytic model for the spatial clustering of dark matter haloes. *MNRAS*, 282:347–361, September 1996.

P. Natarajan and V. Springel. Abundance of Substructure in Clusters of Galaxies. *ApJ*, 617: L13–L16, December 2004. doi: 10.1086/427079.

J. A. Peacock and A. F. Heavens. Alternatives to the Press-Schechter cosmological mass function. *MNRAS*, 243:133–143, March 1990.

P. J. E. Peebles. *The large-scale structure of the universe*. Princeton Univ. Press, Princeton, N.J., 1980.

Planck Collaboration, P. A. R. Ade, N. Aghanim, C. Armitage-Caplan, M. Arnaud, M. Ashdown, F. Atrio-Barandela, J. Aumont, C. Baccigalupi, A. J. Banday, and et al. Planck 2013 results. XVI. Cosmological parameters. *ArXiv e-prints*, March 2013.

W. H. Press and P. Schechter. Formation of Galaxies and Clusters of Galaxies by Self-Similar Gravitational Condensation. *ApJ*, 187:425–438, February 1974. doi: 10.1086/152650.

R. K. Sheth and G. Tormen. Large-scale bias and the peak background split. *MNRAS*, 308:119–126, September 1999. doi: 10.1046/j.1365-8711.1999.02692.x.

P. Valageas. Impact of a warm dark matter late-time velocity dispersion on large-scale structures. *Phys. Rev. D*, 86(12):123501, December 2012. doi: 10.1103/PhysRevD.86.123501.

This preprint was prepared with the AAS LaTeX macros v5.2.